POLITECNICO
MILANO 1863

SCUOLA DI INGEGNERIA INDUSTRIALE
E DELL'INFORMAZIONE

Executive Summary of the Thesis

Analysis of degradation of lithium-ion batteries coming from real automotive application

Laurea Magistrale in Energy Engineering - Ingegneria Energetica

Author: Gian Marco Trippetta

Advisor: Prof. Claudio Rabissi

Co-advisor: Ing. Gabriele Sordi

Academic year: 2021-2022

1. Introduction

Lithium-ion batteries constitute the bulk of the portable energy storage sector. Extensive research has been carried out in recent years as this technology could enable for further improvements in many of the energy challenges the world is facing right now. The comprehension of physical and chemical mechanisms interplay behind cells degradation will be the focus of this work. Experimental measurements will be taken on multiple samples aged in a real hybrid automotive application before being interpreted with the support of research literature and of a physical model developed in parallel. The latter allows for the identification and quantification of the nature and extent of the main degradation modes in Li-ion cells through the calibration of a small set of parameters. The topics that will be developed in this work are the following:

Chapter 1: description of the state of the art of lithium-ion battery technology with focus on lithium iron phosphate batteries (LFP) and its degradation modes.

Chapter 2: the testing station alongside the experimental techniques involved in this work are presented and characterized. Moreover, the physical model and the calibration algorithm are introduced.

Chapter 3: results of experimental tests on Beginning of Life (BoL) cells are reported and interpreted in order to establish the most significant measures to formulate a protocol for the characterization of the cells. Thus, the physical model is used alongside the calibration algorithm to quantify pristine cells parameters.

Chapter 4: End of Life (EoL) battery samples are tested and compared with BoL results, allowing for the analysis of residual performances and the interpretation of the occurred degradation mechanisms. Moreover, an optimization algorithm is introduced for the quantification of the main degradation parameters.

Chapter 5: deepening on the behaviour of cells in parallel configuration in preparation for future studies on non-invasive diagnostic methods for battery modules.

2. State of Art

2.1. Lithium-ion batteries components and operation

Lithium-ion batteries (LIB) are an electrochemical device that can store electric energy as chemical energy and allow the conversion from one another exploiting the reduction – oxidation reactions of lithium ions (see Chapter 2). The structure of a LIB is that of a system made of two different electrodes, interacting by means of a non-aqueous electrolyte and a separator that allow the transport of Li-ions between them while inhibiting the flow of electrons which would cause short circuits. Meanwhile the two current collectors, in aluminum (positive) and copper (negative) respectively, gather the electrons pro-

duced by the electrochemical reactions in the electrodes and allow for an external flow of electrons in a circuit connected to a load/charger. For the purpose of this work the main focus will be the lithium iron phosphate chemistry (LFP) being the sample analyzed in the experimental campaign.
Since LFP first appeared in 1997, its chemical features have been thoroughly analyzed in literature. Its main drawback is the limited theoretical energy density ($\sim 170\ mAh/g$ capacity respect $\sim 285\ mAh/g$ of a $LiMnO_2$ cathode), while it owns an ordered olivine structure characterized by small distinctions between the lithiated and de-lithiated states which is the main cause of ita characteristical features (see Chapter 2.1). Graphite instead is the constituent of the negative electrode, widely used in commercial applications, its characterized by four distinct stages during the lithium intercalation process which are clearly visible in experimental measures (see Chapter 2.1).

2.2. Degradation modes

Degradation in LIB is caused by a large number of physical and chemical mechanisms [2] (see Chapter 2.2). Moreover, the different causes, rates and interdependencies of these degradation mechanisms make them extremely challenging to model, which is why most physics-based models focus only on the most dominant mechanisms, such as the formation and growth of the solid electrolyte interphase (SEI), a passivation layer that inevitably form on graphite, resulting in a loss of capacity and power of the battery. In this work, the dual-tank model was selected, as a simple but yet accurate approach for the description and quantification of the main LIB degradation mechanisms. Therefore, three main characteristic parameters will be presented [1, 5]:

- **Loss of Lithium Inventory** (LLI) groups mechanisms resulting in a reduction of the amount of cyclable lithium available like SEI growth and formation;
- **Loss of Active Material** (LAM), occurring in both positive (LAM_p) and negative (LAM_n) electrodes, it groups mechanisms that lead to a reduction of the active sites available for lithium intercalation like anode and cathode dissolution, metal deposition or lithium plating.

3. Methodology

3.1. Battery samples

The LIB samples used in this research work are the cylindrical LFP cells A123 ANR26650 M1A and the A123 ANR26650 M1B (see Chapter 3.1). Their main difference, which was confirmed by geometrical measurements performed on both samples, is the active area of the electrodes: 0.1690 m^2 for M1A (2.3Ah) and 0.1852^2 for M1B (2.5Ah).

The samples were supplied by a private company and comprehended both new as well as aged cells which were employed in real automotive operation. Type M1B cells were the only ones available in pristine conditions and 17 of them were tested for a complete mapping of their characteristics. The other share of cells instead were mostly of M1A type and in total 40 different samples were tested.

3.2. Experimental techniques

With the aid of an experimental station improved with respect to the previous thesis work [3], a selection of measurements at specific operating conditions have been chosen to describe the battery samples functioning and their degradation state. These are listed here below (see Chapter 3.3):

- **Charge and discharge** focus on the relation between the cell voltage and the charge exchanged during the test. Being strongly influenced by the test operating conditions (C-rate and temperature), they allow for the understanding of the cell sensitivity with respect to those parameters [1];
- **Incremental Capacity** (IC) and **Differential Voltage** (DV) are defined as the partial derivative of exchanged charge with respect to voltage and its opposite during the discharge of a battery. These two curves are mainly obtained from close to equilibrium discharge curves at 0.1C, 25°C, were kinetic effects can be neglected. Therefore, they highlight the thermodynamic characteristics of of lithium de-/intercalation in the electrodes, that during the battery operation undergo a sequence of single-phase regions and phase transitions, that correspond to different slopes of the discharge curve [1];
- **Pulse power test** consist in a constant current pulse, at a controlled temperature of 25ºC with power measured at 4 main timesteps (2s, 10s, 18s and 30s). The procedure is then repeated in both discharge and charge for a multiple C-rate values, in our case up to 12.5C (= 31.25A) with 2.5C steps;
- **Electrochemical Impedance Spectroscopy** (EIS), is a tool widely studied in literature [4, 6] which consist in the measure of the impedance of the cell at different frequencies by the superimposition of a sinusoidal current I with frequency f on a steady state condition, while recording the voltage response V. Therefore, different mechanisms are stressed as function of their characteristic time, by varying the frequency of the perturbation. Three of them will be isolated and analyzed in this work: ohmic effects, also known as high frequency resistance (HFR), charge transfer phenomena (R_{ct}, mid frequency) and diffusion phenomena (R_w, low frequency).

3.3. Physical model

A pseudo-two-dimensional electrochemical model (P2D) with the addition of a 2D thermal component, developed in *COMSOL Multiphysics®*, was taken from the previous thesis work of the same research track [3] but it was then adapted and optimized for the specific application on LFP batteries. The model includes the material balance in the electrolyte and in the electrodes, the Butler-Volmer electrochemical kinetics, the charge conservation in the electrolyte and in the electrode, and the double layer charge or discharge (see Chapter 3.4).

3.4. Optimization algorithms

An Adaptive Particle Swarming Optimization algorithm (APSO) was implemented alongside the physical model, as a tool for an effective calibration of the parameters that characterize the kinetic behaviour of the battery (*see Tab. 2*). This consists in a population-based optimization tool in which the members of the population, named particles, can move in a n-dimensional space, where n is the number of parameters that has to be calibrated. There, they move driven by the minimization of an objective function defined as the difference between the experimental curve used for the calibration (see diagnostic protocol in *Tab. 1*) and the one produced by the model.
While for the calibration of pristine cells, the thermodynamic parameters (TDN in *Tab.2*) are kept as equal to zero, in aged cells, degradation mechanisms have to be accurately modelled. Therefore, an additional model able to estimate those parameters was developed. Thanks to the close to the equilibrium state, of the so called slow discharge (C/10, 25°C) (*see Section 3.2*), it was possible to isolate the calibration of the thermodynamic parameters with a model that, with help of a PSO algorithm, reproduces the experimental discharges by matching the equilibrium curves of the electrodes.

4. Beginning of Life samples

4.1. Experimental testing

The experimental testing on BoL cells was performed in order to gather a significant amount of measurements, to be then selected and used for the formulation of the diagnostic protocol alongside with direct comparisons with curves of aged cells. Therefore, all the measurements listed in *Section 3.2* were performed at multiple operating conditions. Moreover by a combination of two EIS for the calibration of parameters group KIN_1 and two discharges for the calibration of parameters group KIN_2, the following protocol was conceived:

Measure	C-rate [1/h]	SoC [%]	DoD [%]	Temp. [°C]
EIS	-	100	-	25
Discharge	10	100	50	25
EIS	-	50	-	10
Discharge	1	50	50	10

Table 1: *Measurements for degradation diagnosis protocol. (EIS performed for frequencies ranging from 0.02Hz to 20kHz)*

4.2. Kinetic parameters calibration

Once the four representative curves constituting the characterization protocol (*see Tab. 1*) were obtained experimentally, it was possible to proceed with the calibration of the kinetic parameters (*see Tab. 2*) through the APSO algorithm. During each of the two steps (KIN_1 and KIN_2) 25 particles per calibrated parameter were initialized, in order to start with a good amount of heterogeneous solutions. The time required for finding a solution in 10 iterations (good benchmark for convergence) was approximately 45 hours for the first step and 18 hours for the second one. In the end, the calibrated parameters (*see Tab. 2*) were able to replicate with good approximation the discharge curves for a very wide range of C-rates (up to 10C) while the dependency on temperature was good for high C-rates but underestimated for low ones (1C). EIS measurements instead, showed good dependency of temperature on the charge transfer phenomena but a bed response in terms of HFR whose variation was overestimated by the model.

5. End of Life samples

5.1. Samples selection

The samples available for the research study where chosen among three battery packs, and were supplied in modules, each made out of 96 batteries arranged as a series of 12 smaller packs (numbered as string 1 to 12) each consisting in a parallel of 8 cells. The selection of these samples was performed accordingly to information provided by the so called LOGfiles. These are collections of diagnostic data acquired and organized by the battery management system (BMS) of each battery pack. The objective of this first analysis was to understand if, by gathering all the information about operating conditions, age of the samples or any other heterogeneity, it was possible to cross check this data and give an estimate of the State of Health (SoH) of the cells.

	Symbol	Value Range	Calibrated value
KIN$_1$	k_{pos} [−]	$[5e-12\,;5e-9]$	3.67e-11
KIN$_1$	k_{neg} [−]	$[5e-12\,;5e-9]$	3.64e-09
KIN$_1$	$C_{dl,pos}$ $[F\,m^{-2}]$	$[0.05\,;20]$	1.56
KIN$_1$	$C_{dl,neg}$ $[F\,m^{-2}]$	$[0.05\,;20]$	0.21
KIN$_1$	$EA_{k,neg}$ $[J\,mol^{-1}]$	$[20000\,;60000]$	52562
KIN$_2$	cond$_{el}$ [−]	$[0.05\,;1]$	0.11
KIN$_2$	diff$_{el}$ [−]	$[0.05\,;1]$	0.38
KIN$_2$	$D_{s,pos}$ $[m^2\,s^{-1}]$	$[5e-18\,;1e-14]$	2.98e-17
KIN$_2$	$D_{s,neg}$ $[m^2\,s^{-1}]$	$[1e-16\,;1e-13]$	1.46e-15

Table 2: *Optimized parameters for BoL M1B cell calibration.*

Therefore, the first step consisted in a categorisation of the modules based upon three simple indicators listed here:

- Year of production
- Total amount of measurements: an indicator of the actual usage of the battery modules;
- Status assessment: BMS notification of module replacement because of operations out of the desired conditions.

Despite all the available packs were put into operation in 2013, the largest share of modules was manufactured in 2018 while few in 2013 and only one in 2016. More importantly, it was noticed that the relation between age and status level is not univocal: several 2013 modules still provide "no assess" status, while several 2018 modules do. Another important information which was provided within the diagnostic data are temperature measurements, presented as the total amount of sampled events at a certain temperature, discretized into 5^{o}C bands. Temperature sensors are two per module, in contact with two cells and are located at the bottom and on top of the module close to the air flow inlet and outlet, respectively. This highlighted vertical temperature differences between the two measures, which should be carefully considered being a potential driver of heterogeneous aging. The last useful measurement found in the LOGfiles is the pack load current. Its distribution showed that the packs usually operate at currents below |20 A| (C-rate $\approx$ 8C), with an highly recurrent discontinuity peak at about 6.25 A ($\approx$ 2.5C) for discharge, and an highly frequent value at (-)1.25 A ($\approx$ 0.5C) for charges. Unfortunately, more qualitative evaluations were not possible due to the lack of additional information like time references, which could have allowed the understanding of evolution of performances with ageing.

Following the comparison among all the different modules, the decision was to focus the experimental campaign on a module which could highlight multiple effects. For this reason a 2013 module made up of strings with a wide variety of number of status assessment conditions, was chosen.

5.2. Experimental testing

Before starting the testing campaign every cell within each string was numbered in consistence with its relative position in the module, like showed in *Figure 1b*, where the vertical flow of cooling air is indicated. Therefore, the first indication on the degradation state of the string was given by residual capacity measurements (*see Fig. 1a*), resulting in an unexpected heterogeneous distribution of performances, ranging from 55% to 78% with respect to the nominal 2.3 Ah. The best performances were found in the bottom cells with a clear progression of degradation following the vertical direction. Moreover, as the cooling system provided air from below, this effect could have been caused by an uneven temperature distribution along the vertical direction.
IC and DV curves were obtained from slow discharges as a tool for highlighting the thermodynamic characteristics of the electrodes. Differential voltage curves (*see Fig. 2b*) highlight a mismatch between pristine and aged cells related to the almost complete loss of valley **1** and to the shrinking of the second one (see Chapter 4.1). As stated in the works by Li *et al.* [5] and in the works by Sarasketa-Zabala *et al.* [7], occupation of stages 2 and 3 sites is thermodynamically favoured with respect to stage 1. Therefore, the reduction of the first voltage plateau must be attributed to LLI which is often caused by SEI formation. While reductions in stages 2 and in this case mainly 3, cannot be explained solely by the same mechanism. Thus, apart from the reduction of active lithium, graphite active material was apparently modified, as showed up by the peak shifting effect in stage 3. This peak gradually moves to the right as

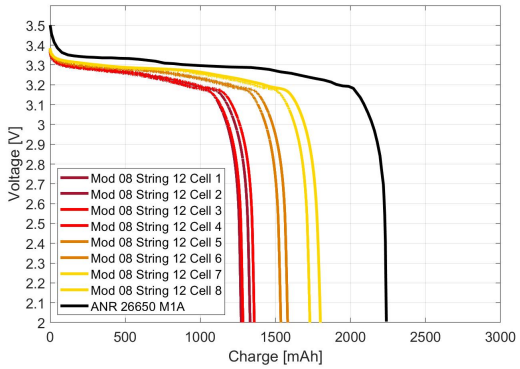

(a) *Discharge at 0.1C, 25°C for the capacity retention test.*

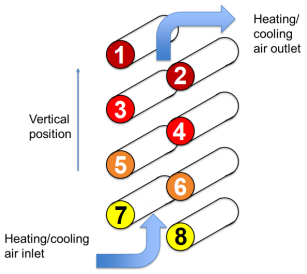

(b) *Numeration logic of each cell in a string.*

Figure 1

we consider more degraded batteries, meaning that less charge is stored and hence an higher LAM could be found. Incremental capacity curves (*see Fig. 2a*) varied accordingly to the DV curves valleys, with the first peak (related to high SoC) almost entirely disappearing. The second peak instead, shows a significant reduction with respect to the BoL case and indicates a downward trend with ageing. Unfortunately, being the IC curve of M1A cell obtained from a C/5 discharge it is not possible to compare the position of the peaks. Moreover, the same comparison can be performed on the aged cells only, revealing a peak shifting effect towards lower voltages with performance worsening, thus giving an indication on the increase of internal resistances [1].

As expected, all EIS measurements (see Fig 3) showed higher impedances in aged cased with respect to the BoL ones. Moreover, all cells show a pure resistive increase (HFR) which, accordingly to Sarasketa-Zabala *et al.* [7], indicates degradation of electrolyte that leads to growth of SEI layer (LLI). In the mid-frequency region instead, where a clear growth of the semicircle is displayed, the worsening of the kinetics of the charge transfer is often considered as the main phenomena. Moreover, the work by Iurilli *et al.* [4], presents many causes behind the growth of the mid-frequency arch. Namely SEI growth and degradation (LLI), Graphite degradation (LAMn) and finally Cathode Electrolyte Inter-

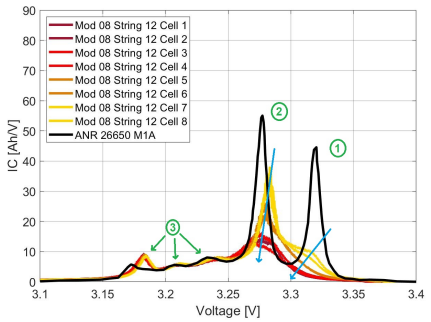

(a) *Incremental capacity*

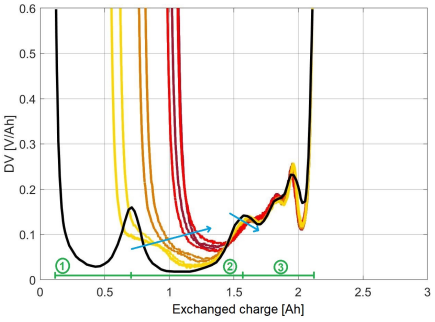

(b) *Differential voltage*

Figure 2: *Incremental Capacity (IC) and Differential Voltage (DV) from discharge at 0.1C, 25°C of string 12 module 8 compared with M1A BoL case taken from C/5, 25°C discharge in [7]. Differential voltage curves are aligned with respect to last valley.*

face (CEI) formation and electrode particle cracking (LAMp) . Concerning low-frequencies instead, effects are very limited as the diffusion branch is often solely shifted towards the right due to the combined effects of the previously analyzed phenomena.

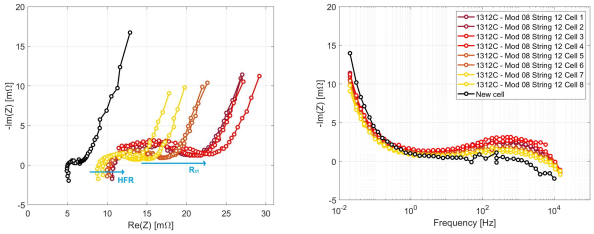

(a) (b)

Figure 3: *Electrochemical Impedance Spectroscopy test at SoC = 100%, 25°C. (a) Nyquist plot, (b) Bode plot of the Imaginary component.*

Finally, the residual power test, more significant from a power intensive application, showed very good residual performances in the discharge phase. All the cells were capable of providing 10C or 12.5C in discharge for 30s which seem promising for second life applications. Anyway, as this is not the main fo-

cus of the research work, batteries second life will not be treated. Finally, the same effect of the vertical positioning of the cells is found from this measure.
The experimental testing was not limited to an 8 cells sample, whereas up to 40 cells were tested throughout the entire campaign. This comprehends a string without any 'assess' conditions which showed similar results but with less heterogeneous performances within the parallel. Moreover, two strings with similar operational characteristics were analyzed for testing the variability of the measurements and finally one 2016 string which showed performances very close to BoL and hence prevented any testing on 2018 modules (see Chapter 5.2).

5.3. Interpretation of thermodynamic degradation parameters

The calibration of the thermodynamic parameters, namely LLI, LAMn, LAMp was performed upon the slow discharge curves (0.1C, 25°C) (see Fig. 1a), which are assumed to be in close-to-equilibrium state, and hence not affected by kinetic effects. Thus, multiple sets of parameters, were obtained as showed in *Table 3*. From the interpretation of the results it was clear that while LLI and LAMn vary accordingly to the experimental measurements results, LAMp has a limited effect that is not quantifiable from these curves. Thus, only LLI and LAMn were furtherly evaluated. In accordance to the works by Sarasketa-Zabala *et al.* [7], it was found that while both parameters increase as the residual capacity is reduced, the relative weight of LAMn over LLI is not constant, with the former indicator growing more than the latter (*see LAMn/LLI in Tab. 3*). This could indicate that due to an uneven efficacy of the cooling sistem or to a more advanced degradation state, at some point the dominant degradation mechanism changes from solely LLI to a combination of LLI and LAM. A similar result is obtained by Dubarry *et al.* in [1] where, by performing dynamic stress tests to a set of LFP batteries, a recurring inflection point, after which degradation significantly increased, was found. LAMn was identified as the major contributor of this phenomena while lithium plating was accounted as the underlying aging mode inducing it.

Module 8 String 12	Residual capacity [mAh]	LLI	LAMp	LAMn	LAMn/LLI
1	1272	0.439	0.032	0.308	0.701
2	1332	0.418	0.209	0.279	0.669
3	1360	0.401	0.013	0.262	0.653
4	1284	0.433	0.000	0.305	0.704
5	1537	0.331	0.173	0.169	0.510
6	1582	0.305	0.001	0.142	0.466
7	1800	0.207	0.065	0.006	0.031
8	1730	0.241	0.132	0.059	0.245

Table 3: *Residual capacities of both strings 02 and 12. The value in percentage is relative to the nominal capacity of 2.3Ah of a M1A pristine.*

6. Tests of cells in parallel configuration

The objective of this final chapter is to find some relations between single cell and parallel of multiple cells measurements, in preparation for future studies on non-invasive diagnostic methods for battery modules.
First, EIS was performed by the Autolab potentiostat on all the strings of Module 08 as well as on a BoL one. This allowed for a direct comparison between the single cell spectra and the one of an 8 cell parallel. However, it was shown that, with good approximation, it is possible to move from one measure to the other by means of a simple equivalent impedance calculation and therefore link the spectra of single cells to the one of the string. Moreover, it was still not possible to identify a way to quantify heterogeneity of performances within the same string.
The second step aimed at the reproduction of the operational functioning of a parallel of cells. Thereafter, a simple numerical model, accounting for charge and voltage balances across the parallel, was developed to estimate voltage and current flows in slow discharges. Experimental measurements were performed on three different configurations made of four new cells, four aged ones and a mixed case with only one aged cell. The measurements taken were slow discharges at 0.1C, 25°C to evaluate residual capacity of the cells and power pulse tests at 7.5C, 25C° to evaluate possible temperature gradients differences.
Figure 4a shows discharge curves of the three tested parallel configurations. The results indicate that the residual capacity is, with good approximation, representative of the sum of the single cells capacities. Moreover, currents distribute themselves during operation accordingly to *Figures 4b, 4c* where we can see that the new/less aged cells always take the biggest share of load. To confirm such a modelling, pulse test were performed to study single cells temperature gradients. As expected, despite lower re-

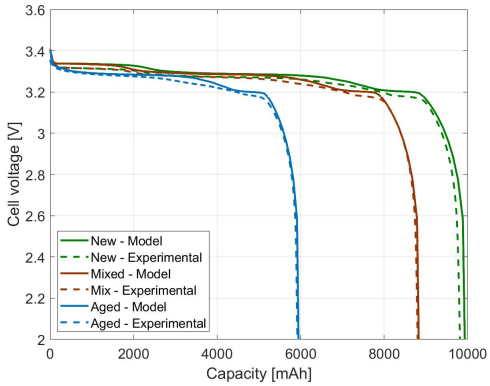

(a) *Voltage profiles of the three different configurations discharge curves at 0.1C, 25°C combined with numerical model predictions.*

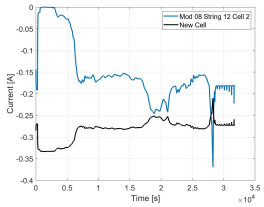

(b) *Current profile of each cell in the Mixed conditions parallel.*

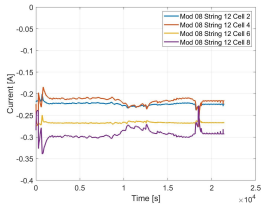

(c) *Current profile of each cell in the Aged conditions parallel.*

Figure 4: *Slow discharge experimental results, combined with model interpretation of current and voltage profiles.*

sistances, less degraded cells were the ones heating more. Moreover, as the pulse was limited to 7.5C due to limitations of the testing station, the temperature differences are too limited to be considered a clear proof.

7. Conclusions

The aim of this research work is the understanding of the degradation mechanisms during real automotive operations and the identification of the stressors that influence the most capacity and performance fades. On top of that, develop a methodology for the calibration of parameters that, thanks to a physical LIBs model, characterize the cell both at beginning and end of life. The main goals achieved in this project are the following:

- Starting from the methods developed in previous thesis works [3], a new protocol for testing and diagnostic of LFP batteries was developed. In a similar way, the methodology for kinetic parameters calibration was adapted from the one used in the previous thesis works [3] while for thermodynamic parameters, a new PSO algorithm able to quantify LLI, LAMn and LAMp by reproducing close to equilibrium curves was implemented;
- A comprehensive experimental testing campaign was carried out enabling the complete characterization of BoL cells from a variety of aspects. Thus, End of Life cells were tested alongside and described by comparison with respect to pristine ones. Residual capacity tests allowed for the understanding of a clear effect of sub optimal thermal management. DV and IC curves showed effects related to both LLI and LAM while EIS displayed worsening of the HFR and of the charge transfer phenomena;
- The calibration of the kinetic parameters was performed on the beginning of life cells but unfortunately due to time limitations it was not extended to EoL samples. On the other hand, the thermodynamic parameters were obtain for all the EoL samples giving additional insights on degradation modes. In particular it was found that cases with worst degradation are driven by both LLI and LAMn, while in cells with better performances, the problem seems almost solely dependent on LLI. Similar effects were obtained in works by Dubarry *et al.* [1] which motivated it as caused by lithium plating. On the other hand LAMp was acknowledged as negligible for values below 20% thank to a sensitivity study on the parameter;
- Lastly a deepening on the diagnostics of parallels of cells was performed as a first step towards the understanding of module testing methods. Experimental measurements on parallels confirmed that is possibility to retrieve averaged information on single cells. Slow discharge measurements were coupled with a simple model capable of reproducing the behaviour of such a configuration, to reproduce the instantaneous current distribution of the cells, showing that the bigger share of current is always taken by less degraded cells and that from a slow discharge curve it is possible to retrieve the sum of the single battery capacities.

Overall, the testing campaign gave a good understanding of the cells conditions after real automotive operation. This include effects already known from lab testing with the addition of some unexpected heterogeneity related to operation. Still many points remain open for further development:

- Carry out experimental measurements on cells with different operational stressors (different battery pack) to quantify the variability of the results with respect to this work;
- Calibration of the EoL cells kinetic parameters for the understanding of additional ageing phenomena that could explain the incerase in resistance and the loss of power. This results could be furtherly enhanced if the LIB model was improved on working with wide ranges of C-rate and temperatures;

- A cycling and a calendar campaign could be performed on both BoL and EoL samples to understand if laboratory-induced degradation is comparable and eventually which of the two types of degradation campaigns is predominant as well as to evaluate future margins of usage for second life applications. This test were actually started mid-September but as results are still very preliminary, they were not included in this work;
- Finally the study the parallel configuration could be improved in many different ways, for instance with the formulation of a new methodology, implementation of a physical model and a measure representative of the cells heterogeneity within a single string.
- Introduce ex-situ/coin cell measurements to validate the interpretation on degradation modes.

References

[1] D Anseán, M Dubarry, A Devie, BY Liaw, VM García, JC Viera, and M González. Operando lithium plating quantification and early detection of a commercial lifepo4 cell cycled under dynamic driving schedule. *Journal of Power Sources*, 356:36–46, 2017.

[2] Christoph R Birkl, Matthew R Roberts, Euan McTurk, Peter G Bruce, and David A Howey. Degradation diagnostics for lithium ion cells. *Journal of Power Sources*, 341:373–386, 2017.

[3] A. Rondi D. Conti. Experimental investigation of lithium-ion battery automotive related aging and model-based interpretation. Master's thesis, Energy Engineering, 2020-21.

[4] Pietro Iurilli, Claudio Brivio, and Vanessa Wood. On the use of electrochemical impedance spectroscopy to characterize and model the aging phenomena of lithium-ion batteries: a critical review. *Journal of Power Sources*, 505:229860, 2021.

[5] Dongjiang Li, Dmitri L Danilov, Barbara Zwikirsch, Maximilian Fichtner, Yong Yang, Rüdiger-A Eichel, and Peter HL Notten. Modeling the degradation mechanisms of c6/lifepo4 batteries. *Journal of power sources*, 375:106–117, 2018.

[6] Mohamed Abdel Monem, Khiem Trad, Noshin Omar, Omar Hegazy, Bart Mantels, Grietus Mulder, Peter Van den Bossche, and Joeri Van Mierlo. Lithium-ion batteries: Evaluation study of different charging methodologies based on aging process. *Applied Energy*, 152:143–155, 2015.

[7] E Sarasketa-Zabala, I Gandiaga, E Martinez-Laserna, LM Rodriguez-Martinez, and I Villarreal. Cycle ageing analysis of a lifepo4/graphite cell with dynamic model validations: Towards realistic lifetime predictions. *Journal of Power Sources*, 275:573–587, 2015.